American Scientific Research Journal for Engineering, Technology, and Sciences (ASRJETS)
ISSN (Print) 2313-4410, ISSN (Online) 2313-4402

http://asrjetsjournal.org/

Brief Review on Iron-Based Superconductors Including Their Characteristics and Applications

Md. Atikur Rahman[a], Md. Arafat Hossen[b]

[a] *Department of Physics, Pabna University of Science and Technology, Pabna-6600, Bangladesh*
Email: atik0707phy@gmail.com

Abstract

The recent discovery of iron-based superconductors has evoked eagerness for extensive research on these materials because they form the second high-temperature superconductor family after the copper oxide superconductors and impart an expectation for materials with a higher transition temperature (T_c). It has also been clarified that they have peculiar physical properties including an unconventional pairing mechanism and superconducting properties preferable for application such as a high upper critical field and small anisotropy. Iron-based superconductors are the new star in the world of solid state physics. The stunning discovery of superconductivity in iron-based materials has exposed a new family of high-temperature superconductors with properties that are both similar to and different than those of the copper-oxide family of superconductors. With transition temperatures approaching the boiling point of liquid nitrogen, these materials promise to provide a rich playground to study the fundamentals of superconductivity, while advancing the prospects for widespread technological applications. In this review paper we have studied the iron-based superconductors, their classifications, different properties and applications.

Keywords: Iron-based superconductors; Properties of iron-based superconductors; Applications

1. Introduction

The phenomenon of superconductivity has a rich and interesting history, starting in 1911 when Kamerlingh Onnes discovered that upon cooling elemental mercury to very low temperatures, the electrical resistance suddenly and completely vanished below a critical temperature T_c of 4 K (-452 °F). This resistanceless state enables persistent currents to be established in circuits to generate enormous magnetic fields, and to store and transport energy without dissipation. Superconductors have other unique properties such as the ability to expel and screen magnetic fields, and quantum oscillations controlled by the magnetic field that provide extraordinary measurement sensitivity. Over the intervening years the number of superconducting materials has grown, with higher critical temperatures and improved metallurgical properties, and these have found their way into a number of technological applications such as MRI imaging systems for the health care industry. But the field

was shocked in 2008 by the surprise discovery of a completely new class of superconductors based on iron. Iron-based superconductors (FeSC) are iron-containing chemical compounds whose superconducting properties were discovered in 2006 by Hosono's group, and boosted in 2008 by the superconducting transition temperature, T_c, of 26 K in $LaFeAsO_{1-x}F_x$. Since then, enormous researches have been done on the materials, with T_c reaching as high as 55 K. These iron-based superconductors have initiated a flurry of activity as researchers try to understand the origin of the superconductivity in these new materials, as well as develop them for prospective use in devices. In this latter context, the new materials have quite high (relatively speaking) superconducting transition temperatures (T_c), and rather favorable current carrying capabilities that should make them useful in practical applications. How does a metal become superconducting? In metals, electrons are free to move and provide electrical conduction, but collisions with other electrons, lattice vibrations, and impurities and defects in the material cause resistance, and thus energy dissipation, in the system. Superconductors circumvent this problem by binding two electrons together into pairs, and these pairs must all move together in a coordinated fashion. If the temperature is low enough there is insufficient thermal energy to break apart and disrupt these pairs, so collisions are not possible and they can move through the material without any interference—resistanceless conductivity. The extraordinary thing about this superconducting pairing is that electrons have the same charge and therefore strongly repel each other. So how can this bound state exist? It took half a century to unravel this mystery, but the pairing occurs for two electrons with equal and opposite speeds, rather than as two electrons "glued together". This unusual state of two electrons in a bound state is called a Cooper pair and is a fundamental property of all known superconductors, including the iron-based ones. A quantitative and complete theory of superconductivity was developed in 1957, which explained that the pairing interaction originated from the lattice vibrations of the solid. This theory provided a thorough understanding for all the superconductors known at the time, and for all the "conventional" superconductors discovered since then. One keystone of this understanding is that any magnetic atoms in the lattice tend to break the Cooper pairs and; therefore magnetism is very detrimental to the superconductivity. However, in 1986 a new class of "high temperature" superconductors was discovered that completely contradicted this rule. These were oxides in which the crystal structure contained sheets of copper and oxygen—called "cuprates" [1]. Oxides typically aren't even conductors let alone superconductors, but more surprising was that the copper ions carry a magnetic spin (like a compass needle), which is the kiss of death for conventional superconductors. Moreover, it turns out that the magnetism is not only tolerated in the cuprates, but appears to play a key role in the Cooper pairing. Up until 2008, all known "high temperature" superconductors exhibited two essential ingredients: copper-oxygen planes of atoms, and magnetic moments on the copper. Hence it was thought that these two properties were essential to achieve "high T_C" superconductivity. Then the iron-based high T_C superconductors were discovered [2, 3]. The atomic structure and bonding of a material controls its properties, and for the iron systems there are four different structure types that have been identified so far, typified by LaFeAsO, $SrFe_2As_2$, LiFeAs, and Fe (Te-Se). The structure for the first two types, which have the highest T_c's, are shown in Figure 1. The common structural feature is a layer of Fe and As atoms (like the Cu-O layer for the cuprates), which is separated by a non-iron layer such as La-O (for LaFeAsO) or Sr (for $SrFe_2As_2$). There are several good reasons why FeSC are so interesting. First, they promise interesting physics that stems from the coexistence of superconductivity and magnetism. Second, they provide a much wider variety of compounds for research and, with their multi-band electronic structure; they offer the hope of finally discovering the mechanism of high

temperature superconductivity and finding the way to increase T_c. Lastly, the FeSC are quite promising for applications. Having much higher H_c than cuprates and high isotropic critical currents, they are attractive for electrical power and magnetic applications, while the coexistence of magnetism and superconductivity makes them interesting for spintronics [15, 16].

In this paper we review iron-based superconducting materials including their characteristics, different properties and some principle applications. We also studied the advantages of iron-based superconductors over high T_C superconductors and cuprate-based superconductors. Table 1 shows the comparison between cuprates and iron-based superconductors. The rest of the paper is organized as follows: in Sec. 2, Iron-based superconductors are given; Sec. 3 contains different properties of iron-based superconductors: Sec. 4 contains applications. Finally, the conclusion is given in Sec.5.

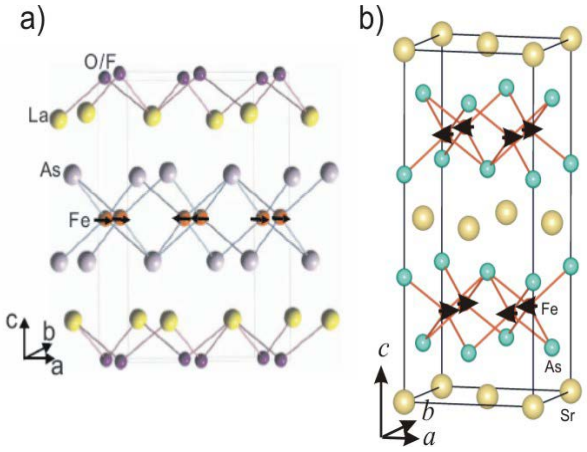

Figure 1: The basic building blocks of the atomic structure for the two types of iron-based superconductors with high critical temperatures T_C: (a) LaFeAsO, and (b) $SrFe_2As_2$. The feature common to the iron superconductors is a metallic layer of iron bonded to arsenic atoms; the iron atoms form a square array with the arsenic atoms above and below the iron plane. The iron-arsenic layer is sandwiched between layers of La-O, or Sr. This basic structural unit is then repeated in all three directions *ad infinitum* to form the macroscopic crystal structure of the material

Table 1: ***Properties of different classes of superconductors***

Property	Conventional superconductors	Copper oxides	MgB_2	Iron-based superconductors
T_c (maximum)	<30 K	134 K	39 K	56 K
Correlation effects	None (nearly-free electrons)	Strong local electronic interaction	None (nearly-free electrons)	Long-range (non-local) magnetic correlations
Relationship to magnetism	No magnetism	Parent compounds are magnetic insulators	No magnetism	Parent compounds are magnetic metals
Order parameter	One band, same-sign *s* wave	One band, sign-changing *d* wave	Two band, same-sign *s* wave	Two band, presumably sign-changing *s* wave
Pairing interaction	Electron-phonon	Probably magnetic (no consensus)	Electron-phonon	Presumably magnetic
Dimensionality	Three dimensional	Two dimensional	Three dimensional	Variable

2. *FeAs-based Superconductors*

Two decades into the intensive study of the cuprate superconductors, the condensed-matter community got stirred up once again when another completely different family of superconductors was discovered by the group of Hideo Hosono in 2006 [4]. The Japanese group reported observation of a superconducting transition in LaFePO at a relatively low temperature of ~ 4K. This original discovery received certain but limited attention from the community. The general excitement came 2 years later when the same group reported superconductivity at a temperature of 26 K, higher that of most conventional superconductors, in a closely related compound $LaFeAsO_{1-x}F_x$ at a doping level of $x = 0.12$ [5], with the parent compound LaFeAsO being non-superconducting at routinely attainable cryogenic temperatures. This latter discovery gave rise to the explosive growth of research of these materials all over the world, which lead to reports of high-temperature superconductivity in several new classes of compounds in this family, such as $SmFeAsO_{0.9}F_{0.1}$ [6] ($T_c \approx 55$ K) and $Ba_{0.6}K_{0.4}Fe_2As_2$ [7] ($T_c \approx 38$ K). Iron-based superconductors started with the discovery of superconductivity at 4 K in LaFePO in 2006, and great interests have been drawn since 2008 when T_c was raised to 26 K in $LaFeAsO_{1-x}F_x$ by replacing phosphorous with arsenic, and some of oxygen with fluorine [3]. So far, iron-based superconductors have been extended to a large variety of materials including four prototypical families of iron-based superconductors, "1111" system RFeAsO (R: the rare earth element) including LaFeAsO [16], SmFeAsO [17], PrFeAsO [18] etc.; "122" type $BaFe_2As_2$ [19], $SrFe_2As_2$ [20] or $CaFe_2As_2$ [21]; "111" type LiFeAs []22-24], NaFeAs [25,26,27] and LiFeP [28], as shown in Figure 2, and further variations such as 42622-type iron pnictides [8-11] and 122-type iron chalcogenides [12-15]. Doping or applied pressure will transform the compounds into superconductivity [29]. A list of oxypnictide and non-oxypnictide iron-based superconductors is given in Table 2.

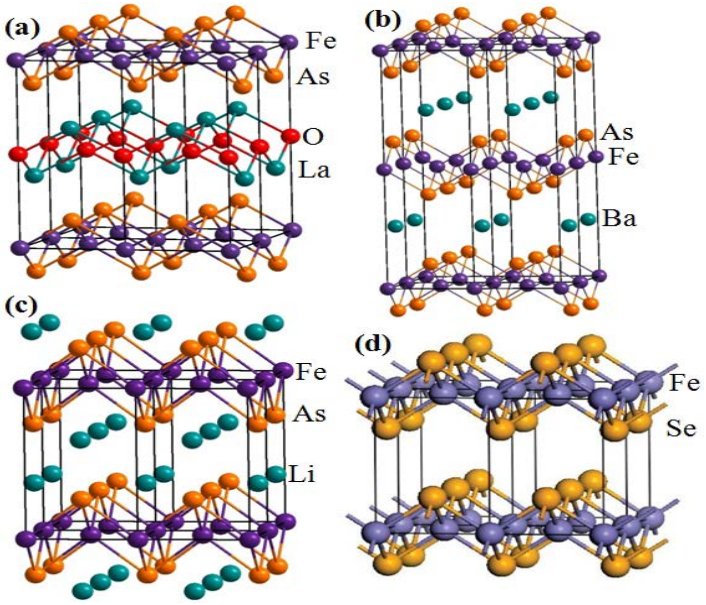

Figure 2: Four families of iron-based superconductors, (a) 1111, (b) 122, (c) 111, (d) 11 types

Table 2: Oxypnictide and Non-oxypnictide Superconductors with transition temperature

Oxypnictide	T_C (K)	Non- Oxypnictide	T_C (K)
$LaO_{0.89}F_{0.11}FeAs$	26	$Ba_{0.6}K_{0.4}Fe_2As_2$	38
$LaO_{0.9}F_{0.2}FeAs$	28.5	$Ca_{0.6}Na_{0.4}Fe_2As_2$	26
$CeFeAsO_{0.84}F_{0.16}$	41	$CaFe_{0.9}Co_{0.1}AsF$	22
$SmFeAsO_{0.9}F_{0.1}$	43	$Sr_{0.5}Sm_{0.5}FeAsF$	56
$La_{0.5}Y_{0.5}FeAsO_{0.6}$	43.1	LiFeAs	18
$NdFeAsO_{0.89}F_{0.11}$	52	NaFeAs	9-25
$PrFeAsO_{0.89}F_{0.11}$	52	FeSe	< 27
$ErFeAsO_{1-y}$	45		
Al-32522 (CaAlOFeAs)	30 (As), 16.6 (P)		
Al-42622 (CaAlOFeAs)	28.5 (As), 17.2 (P)		
$GdFeAsO_{0.85}$	53.5		
$BaFe_{1.8}Co_{0.2}As_2$	25.3		
$SmFeAsO_{\sim 0.85}$	55		

3. *Characteristics and different properties of Iron-Based Superconductors*

1111-type family:

The 1111-type family includes LaFePO and $LaFeAsO_{1-x}F_x$, which are mentioned above, and LnFeAsO with various lanthanide elements (Ln). The atomic structure of the 1111family consists of negatively charged FeP or FeAs layers, where Fe atoms form a planar square lattice, and positively charged LnO layers, as shown in Figure 3(a). With or without doping, electrons are conducting in FeP or FeAs layers. Figs. 4(a) and (b) show that the electrical resistivity of pure LaFePO drops at 4 K and that of F-doped LaFePO drops at higher temperature. These superconducting transitions are confirmed by magnetic susceptibility [Figure 4(c)]. It is noticeable that decrease of the resistivity starts at ~ 10 K in F- doped LaFePO.

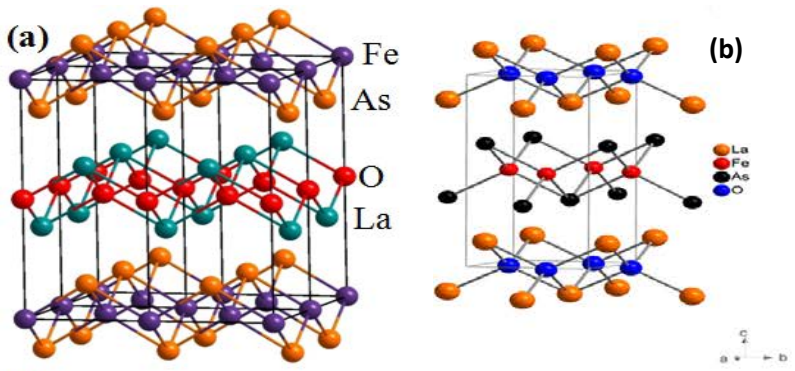

Figure 3: Crystal structures of 1111 (LaFeAsO) type superconductors

Unlike LaFePO, undoped LaFeAsO does not show superconductivity [Figure 5(a)]. With doping of F replacing O in part, $LaFeAsO_{0.89}F_{0.11}$ becomes superconducting. When small pressure is applied to $LaFeAsO_{0.89}F_{0.11}$, T_c increases, reaching a maximum value of T_c = 43 K at 4 GPa, and then it decreases to T_c = 9 K at 30 GPa [30]. At ambient pressure, T_c higher than 40 K is achieved in $SmFeAsO_{1-xFx}$ [31].

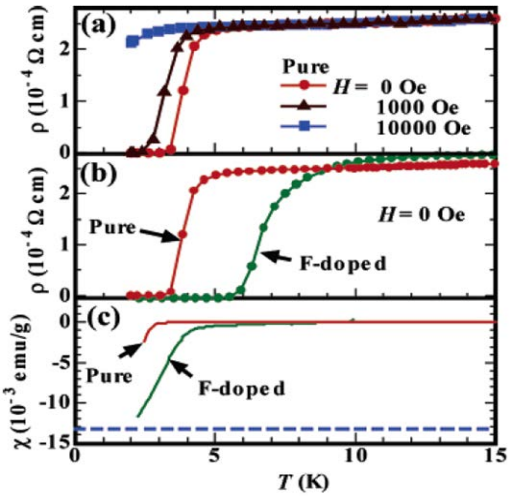

Figure 4: (a) Electrical resistivity, ρ, vs. temperature, T, for pure LaFePO at various magnetic field, H. (b) ρ vs T and (c) magnetic susceptibility, χ, vs T for pure and F-doped LaFePO [32]

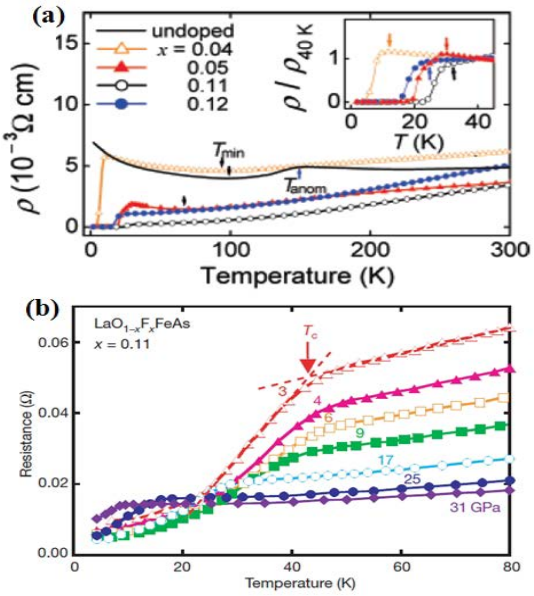

Figure 5: (a) Electrical resistivity, ρ, vs temperature in $LaFeAsO_{1-x}F_x$ for x = 0.0, 0.04, 0.05, 0.11, and 0.12.

(b) Temperature dependence of electrical resistance above 3 GPa in $LaFeAsO_{0.89}F_{0.11}$. The maximum T_c is 43 K at 4 GPa

Reported values of T_c in 1111-type materials include 4 K in LaFePO [2], 26 K in $LaFeAsO_{0.89}F_{0.11}$ [3], 41 K in $CeFeAsO_{0.84}F_{0.16}$ [33], 52 K in $PrFeAsO_{0.89}F_{0.11}$ [34], 54.3 K in $NdFeAsO_{1-y}$ [35], 55 K in $SmFeAsO_{0.9}F_{0.1}$ [36], and 54 K in $GdFeAsO_{1-y}$ [35].

Phase diagram, electronic and superconducting properties of 1111 type superconductors:

The undoped parent compounds of iron-based superconductors are either superconducting or antiferromagnetic at low temperatures. LaFePO, LiFeAs, and FeSe, for example, are nonmagnetic and superconducting even without doping. In contrast, undoped LaFeAsO and $BaFe_2As_2$, for example, are non-superconducting antiferromagnetic metals, and electron or hole doping suppresses the magnetic order and induces superconductivity. The undoped 1111-type iron pnictides show structural and magnetic phase transitions at slightly different temperatures. It is reported by neutron scattering experiments [37] that LaFeAsO undergoes an abrupt structural transition at 155 K, changing from high-temperature tetragonal structure (space group P4/nmm) to low-temperature monoclinic structure (space group P112/n). At ~137 K, long-range antiferromagnetic order starts to develop with a small moment of 0.36 μB per atom and a simple antiferromagnetic ordering of single-stripe type [37], as shown in Figure6. The direction of the Fe magnetic moment was later measured to be longitudinal in the sense that it is parallel or anti-parallel to the antiferromagnetic ordering wave vector [38]. With electron or hole doping, the antiferromagnetic order in the parent compounds is suppressed and superconductivity emerges. Figure 7 shows the typical phase diagram for the 1111-type family which is determined by neutron-scattering measurements on $CeFeAsO_{1-x}F_x$ [39]. The electronic structure of iron-based materials was first studied by S. Lebègue in 2007 using *ab initio* calculations based on the density functional theory (DFT) [36]. The calculated band structure and the Fermi surface of LaFePO are shown in figures 8(a) and (b), respectively. The Fermi surface of LaFePO consists of five sheets, resulting from five bands which cross the Fermi level. Four of the five sheets are cylinder-like along the kz direction reflecting quasi-two-dimensional nature of the atomic structure: two of them are of hole type along the Γ-Z high-symmetry line of the Brillouin zone and the other two are of electron type along the M-A line. The 5th sheet is a distorted hole-type sphere centered at the Z high-symmetry point.

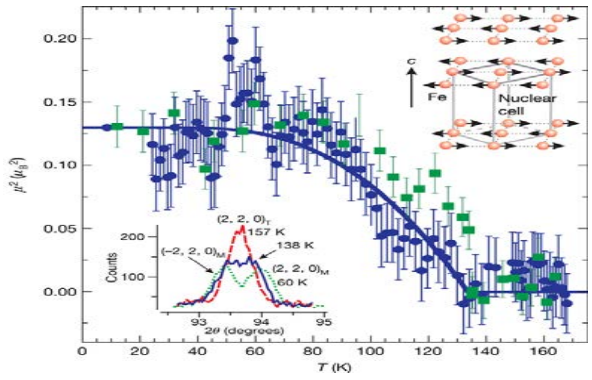

Figure 6: Antiferromagnetic ordering in LaFeAsO. The solid line is a simple fit to mean field theory that gives a Néel temperature T_N = 137 K. The top-right inset shows the single-stripe-type antiferromagnetic ordering of Fe magnetic moments

In Table 3, the superconducting properties of representative iron-based superconductors are summarized. There have been many reports on the measurement of transport properties in magnetic fields for iron-based superconductors using single crystals [40–42]. The most notable feature is their rather high upper critical field (H_{c2}), which is favorable for power applications. For example, the 1111 and 122 type compounds exhibit a very

large slope of $\mu_0 H_{C2}{}^{\|c}$ at T_c of approximately 2–2.5 T/K. The in-plane coherence length ξ_{ab} estimated from $H_{c2}{}^{\|c}$ using the Ginzburg–Landau expression, $\xi_{ab}= [\Phi_0/(2\pi\mu_0 (dH_{c2}{}^{\|c}/dT)|_{Tc} T_c]^{1/2}$, is approximately 1.8–2 nm for the 1111 type compound [40–42]. These values are slightly largerthan those for the copper oxide superconductors with a higher T_c. A small anisotropy factor is very important for the application of superconductors, especially in high magnetic fields. The 1111 type compounds such as NdFeAs(O,F) show a strong temperature dependence of anisotropy evaluated from the upper critical field, $\gamma_H = H_{c2}{}^{\|ab}=H_{c2}{}^{\|c}$, reflecting the anomalous temperature dependence of H_{c2} in both the field directions [48]. The γ_H of approximately 5 at low temperatures is comparable to or slightly less than that of YBCO, while the value near T_c is close to 10. The 1111 type compounds exhibit significant broadening of the resistive transition in high magnetic fields similar to that observed for YBCO, indicating that the irreversibility field H_{irr} is substantially lower than H_{c2}. In Table III, the superconducting properties of representative iron-based superconductors are summarized.

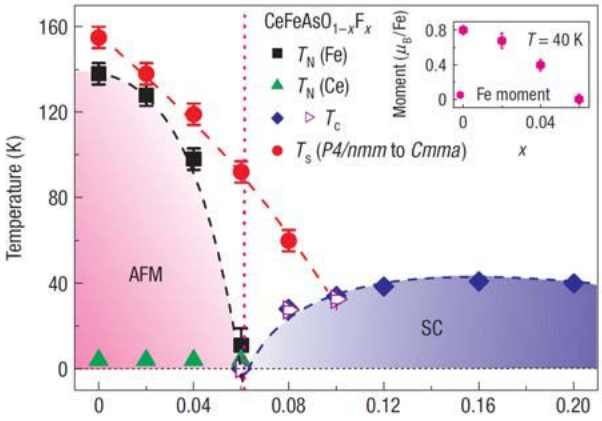

Figure 7: Phase diagram of $CeFeAsO_{1-x}F_x$. The red circles indicate the onset temperature of structural transition. Antiferromagnetic and superconducting phases are marked with AFM and SC, respectively

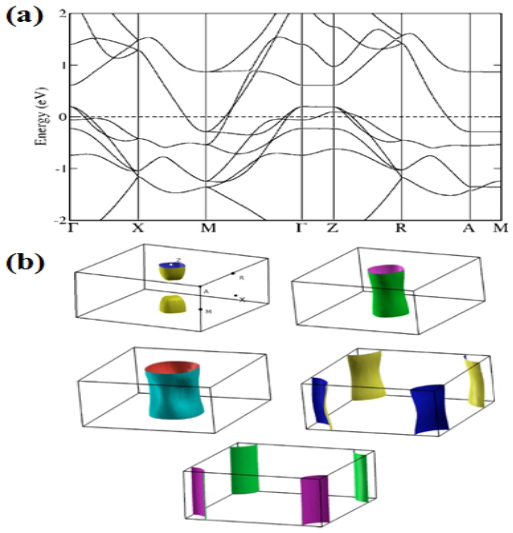

Figure 8: (a) Calculated band structure and (b) the Fermi surface of LaFePO from DFT

Table 3: ***Superconducting properties of representative iron-based superconductors***

Material	T_c (K)	$\mu_o(-dH_{c2}^{\parallel c}/dT\|_{Tc}$ (TK^{-1})	$\mu_o H_{c2}^{\parallel c}(0)$ (T)	Anisotropy factor, γ_H	Coherence length, ξ_{ab} (nm)	ξ_c (nm)	Energy gap, Δ (meV)
RFeAs(O,F) (R = Nd, Sm)	47-55	0.8-2.5	80-100*	5-10	1.8-2.3	0.26	4-7, 10-18
$(Ba,K)Fe_2As_2$	37-38	4-5	70-135*	1.5-2	1.5	1.0	1.8-4.6, 9-11
$Ba(Fe,Co)_2As_2$	22-23	2.5	47-50	1.5-1.9	2.4	1.3	1.9-4.4, 5-7.4
Fe(Se,Te)	14-16	14	~ 50	1.1-1.9	1.2	0.63	~2.3

*Ambiguity exists as described in the text.

122-type family:

Right after discovery of 1111-type family, 122 types ($Ba_{1-x}K_xFe_2As_2$) with T_c of 38 K [43] was found, followed by 111 types (LiFeAs) with T_c of 18 K [44]. The 122- and 111-type families have simpler structures than the 1111-type family. While FeAs or FeP layers are present in 1111-, 122-, and 111-type materials, the 'blocking layer' which separates FeAs or FeP is different for each type: rare-earth oxide or fluoride (for example, LaO or SrF) for the 1111-type family, alkaline-earth metals (for example, Ba) for the 122-type family, and alkali metals (for example, Li) for the 111-type family. Figure 9 shows the 122 type iron-based superconductors. The reported values of T_c in 122-type materials include 38 K in $Ba_{0.6}K_{0.4}Fe_2As_2$ [43], 32 K in $Sr_{0.6}K_{0.4}Fe_2As_2$ [45], 26 K in $Sr_{0.6}Na_{0.4}Fe_2As_2$ [46], and 21 K in $Ca_{0.6}Na_{0.4}Fe_2As_2$ [45]. The structure, composition, dopant species, and T_c values for representative iron-based superconductors are summarized in Table 4.

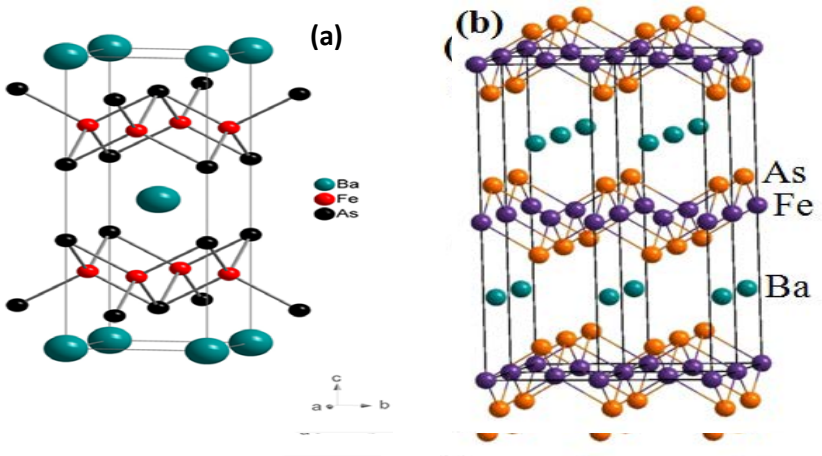

Figure 9: Crystal structures of 122 ($Ba_{1-x}K_xFe_2As_2$) type superconductors

Typical phase diagram and superconducting properties for 122-type family:

A set of experimental phase diagram [47-50] is presented in Figure 10(a) for the Ba-based 122 system, which captures the main traits of 122-type family. In $BaFe_2As_2$, the systematic replacement of either the alkaline-earth metal (Ba), transition metal (Fe), or pnictogen (As) with different elements almost universally suppresses the non-superconducting antiferromagnetic state of parent compounds to asuperconducting nonmagnetic state. This phase transition from the antiferromagnetic state to the superconducting state is generic property of the iron-based superconductor systems which can also be produced by applied external pressure [51]. It is remarkable that the phase diagram of the iron-based superconductor system is very similar to that of copper-oxide materials [52] shown in Figure 10(b), except that the undoped parent compound of copper-oxide materials is an antiferromagnetic Mott insulator.

The 122 type compounds such as $(Ba,K)Fe_2As_2$ and $Ba(Fe,Co)_2As_2$ have a much smaller γ_H of approximately 1.5 at low temperatures, [49] which is comparable to that for MgB_2 and suggests a minimal thermal fluctuation effect. Actually the resistive transition of 122 type compound single crystals exhibits an almost parallel shift of the resistive transition in magnetic fields, [47,49] although slight broadening was reported in $Ba(Fe,Co)_2As_2$ thin films [53]. Table 3 shows the superconducting properties of 122-types in details.

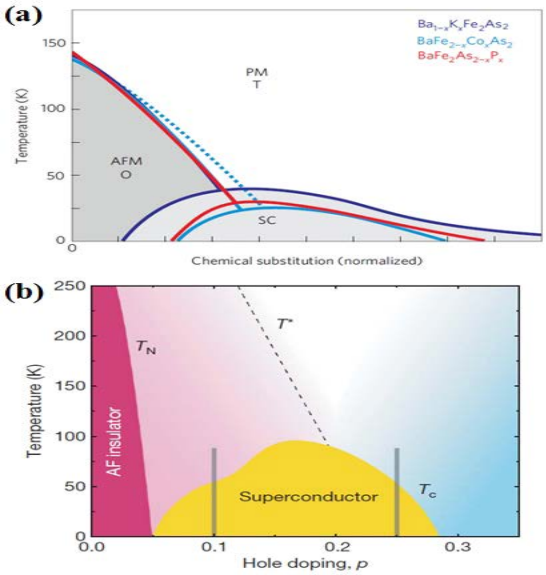

Figure 10: (a) Phase diagram of the $BaFe_2As_2$ system, shown for K [47], Co [31] and P [49] doping. The dotted line indicates tetragonal (T) to orthorhombic (O) structural phase transitions in Co doped samples. (b) Doping dependent antiferromagnetic transition temperature, T_N, superconducting transition temperature, T_c, and pseudogap crossover temperature, T^*, in YBCO [52]

111-type family:

As it is highly reactive with air and, consequently, more challenging to study, the 111 family yields many interesting results. The main representative of the family, LiFeAs, [62, 63] is the most “arpesable” compound [64–66]. It grows in good quality single crystals [67] that cleave between the two Li layers, thus revealing a non-polar surface with protected topmost FeAs layer; it is stoichiometric. The ‘‘111’’ type compounds such as

AFeAs (A: alkaline elements) with the highest T_c of18K [71] have the CeFeSi structure (space group P4/nmm) with each A*e* element of the 122 type compounds substituted by two A*e* elements. The NaFeAs is another member of the 111 family [Fig11]. It shows three successive phase transitions at around 52, 41, and 23 K, which correspond to structural, magnetic, and superconducting transitions, respectively [68,69]. The compound is less reactive with the environment than LiFeAs but exposure to air strongly affects T_c [68]. Replacing Fe by either Co or Ni suppresses the magnetism and enhances superconductivity [69]. For ARPES on NaFeAs, see references [72 and 73]. The reported values of T_c in 111-type materials include 30 K in $K_xFe_{2-y}Se_2$, 18 K in Li_xFeAs, 9 K in Na_xFeAs. The structure, composition, dopant species, and T_c values for representative iron-based superconductors are summarized in Table 4.

Table 4: Structure, composition, dopant species, and T_c values for representative iron-based superconductors

Structure	Composition	Dopant (Site)	T_c (K)
1111	LnFePO (Ln = La, Sm, Gd)		3-7
		F (O)	7
	RFeAsO (R = Y, La-Ho)	F (O)	26-55
		Vacancy (O)	28-55
		Co (Fe)	7-18
122	$AeFe_2As_2$ (Ae = Ca, Sr, Ba)	A (Ae)	20-38
		Co (Fe)	20-23
		P (As)	30
	$K_xFe_{2-y}Se_2$ [a)]		30
111	Li_xFeAs		18
	Na_xFeAs		9
11	$Fe_{1+x}Se$		8 (37[b)])
		Te (Se)	14 (21[c)])
		S (Se)	7
21113	$Sr_2ScFePO_3$		17
	$Sr_2VFeAsO_3$		37 (46[b)])
32225	$Sr_3Sc_2Fe_2As_2O_5$	Ti (Sc)	45

11-type family:

Among the iron-based superconductors 11 type compounds have the lowest T_c. However, their simplest crystal structure and the pressure-induced significant increase in T_c straightforwardly lead to motivation for fabricating epitaxial films on lattice-mismatched substrates, which may show strain-induced T_c enhancement. The 11-type materials are iron chalcogenide, which started with FeSe having T_c of 8 K at ambient pressure [54] and 36.7 K with applied pressure of 8.9 GPa [55]. This family also includes $FeTe_{1-x}Se_x$, and $FeTe_{1-x}S_x$. These materials have the simplest structure among iron-based superconductors, in which iron-chalcogenide layers are simply stacked

together. Reported values of T_c in 11-type materials include 8 K in FeSe at ambient pressure [54] and 36.7 K in FeSe under pressure of 8.9 GPa [23], as mentioned above, and 14 K in $FeTe_{0.5}Se_{0.5}$ [56], 2 K in $Fe_{1.13}Te_{0.85}S_{0.1}$ [57], and 10 K in $FeTe_{0.8}S_{0.2}$ [58]. The 11 type compound also has a γ_H similar to or slightly smaller than that for the 122 type compounds. In spite of such a small γ_H, observation of clear broadening of the resistive transition was reported [48]. The superconducting properties are shown in Table 3. In copper oxide superconductors, the anisotropy factor correlates well with the distance between the CuO_2 planes or the thickness of the blocking layer, that is, a thinner blocking layer leads to smaller anisotropy [60]. This is also the case for the iron-based superconductors. Recently, substantially larger anisotropy was observed for the compounds with a thick perovskite-like blocking layer, and an inverse correlation between the irreversibility fields H_{irr} and γ, as seen in copper oxides, was also reported by Ogino and his colleagues [61].The crystal structures and phase diagram of 11-type superconductors are shown in Figs. 12 & 13 respectively.

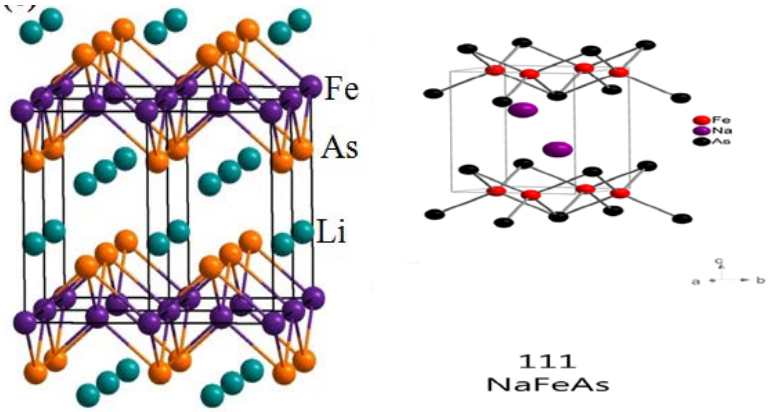

Figure 11: Crystal structures of 111 type superconductors

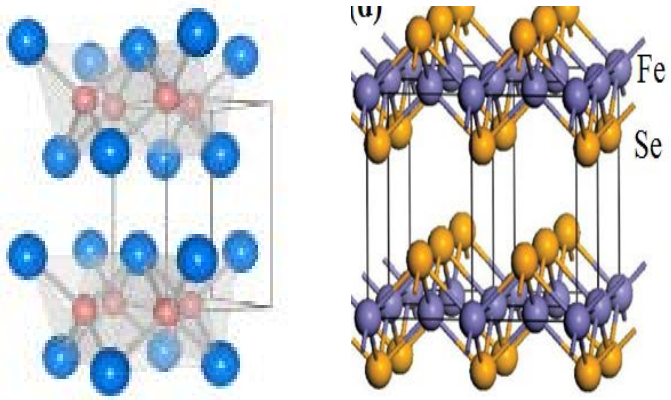

Figure 12: The crystal structures of 11-type superconductors

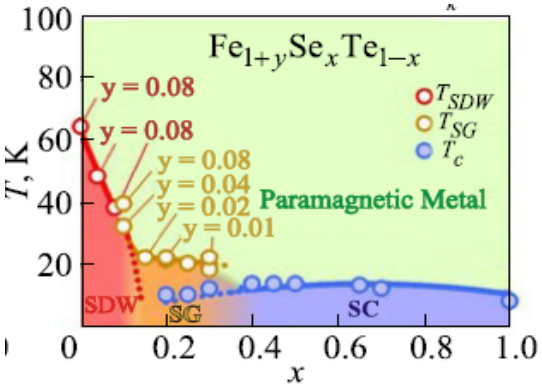

Figure 13: Phase diagram of 11-type SC

4: Applications of Iron-Based Superconductors

4.1 Applications of Iron-based superconductors in wire and tape

The power-in-tube (PIT) method has been applied to the wires fabrication which is based on high-temperature superconductors such as Bi-based copper oxides and MgB_2, and now-a-days km-length commercial wires are available [75]. Soon after the discovery of high-T_c iron-based superconductors, the trial fabrication of F-La1111 and F-Sm1111 wires was reported by Gao and coworkers [76, 77]. They employed an in situ PIT method using La(Sm), As, LaF_3 (SmF_3), Fe, and Fe_2O_3 as starting materials. A Ta tube or a Fe tube with an inner Ti sheath was used to prevent the reaction between the tubes and the 1111 type compounds. After swaging the tubes containing the raw materials and heat treatment at above 1150 ^oC, they obtained a wire as shown in Figure 14. Although they could not observe a high transport I_c, magnetization measurements revealed that the core material of the wire with a T_c as high as 52K had a self-field J_c of approximately 4000 A/cm^2 at 5K and a weak magnetic field dependence of J_c, as shown in Figure 15, indicating an encouraging first step toward fabrication of practical wires. The fabrication of K-Sr122 wires by the PIT method was also subsequently reported by the same group [78]. To obtain a high transport I_c, they improved the wire fabrication process. They employed Ag inner sheath to prevent the reaction with the raw materials and added Ag to the raw materials to enhance grain growth. This improved process led to the successful observation of a transport J_c of 1200 A/cm^2 at 4.2K for K-Sr122 wires [79]. Recently, they employed an ex situ PIT method using K-Sr122 powder and increased the transport J_c to 3750 A/cm^2 at 4.2 K [80]. By employing a similar method and annealing at relatively low temperatures of 850–900^{o}C, F-Sm1111 wires with a transport J_c of 2700 A/cm^2 were also fabricated [81]. Very recently, Togano and his colleagues reported the successful fabrication of Ag-sheathed K-Ba122 wires with a large transport I_c of as high as 60.7A at 4.2 K, which corresponds to a self-field J_c of 1.0 ×10^4 A/cm^2, by an ex situ PIT method with the addition of Ag [82]. As shown in Figure 16, the wires exhibited a transport J_c of 1.1 × 10^3 A/cm^2 even in a field of 10 T. High self-field transport J_c at 4.2K of approximately 4000 A/cm^2 has also been reported for F-Sm1111 wires fabricated by an ex situ PIT method using a binder composed of SmF_3, SmAs, and FeAs [83]. However, further improvement of the transport J_c is required to realize practical wires. Considering the weak-link behavior of high-angle GBs, the texturing of grains in wires appears to be necessary to some extent. Moreover, a recent TEM study on a polycrystalline K-Sr122 sample indicated the existence of nanometer-scale amorphous layers and oxygen enrichment at the grain boundaries [84].

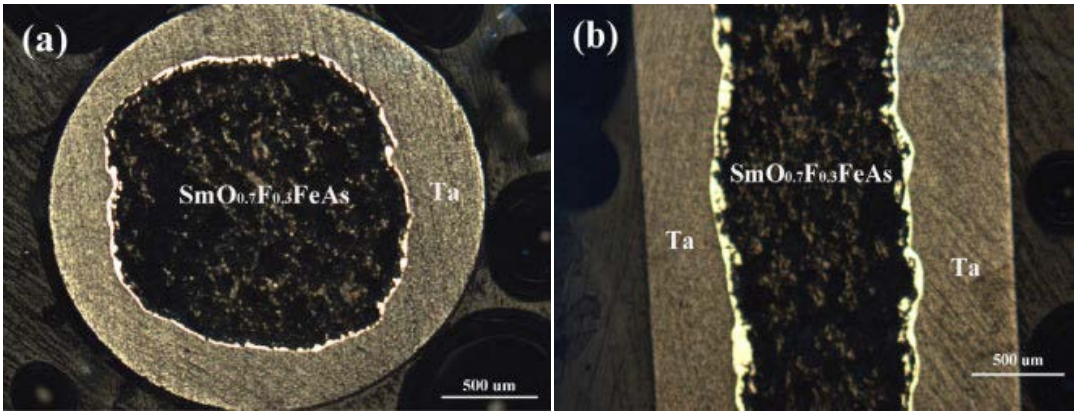

Figure 14: (Color online) Optical images of a typical (a) transverse and (b) longitudinal cross section of the first successfully fabricated $SmFeAsO_{1-x}F_x$ (F-Sm1111) PIT wires after heat treatment

Mizuguchi and his colleagues reported the fabrication of wires based on the 11 type compound Fe (Se,Te) by an in situ PIT method [85]. They reported that the Fe sheath played the role of a raw material for synthesizing superconducting phases as well as the sheath. Their group also reported the fabrication of Fe (Se,Te) wires by an ex situ PIT method and obtained a transport J_c of about 100 A/cm^2 at 4.2 K [86]. Moreover, a higher J_c of approximately 1000 A/cm^2 has recently been reported in FeSe PIT wires by Ozaki and his colleagues [87]

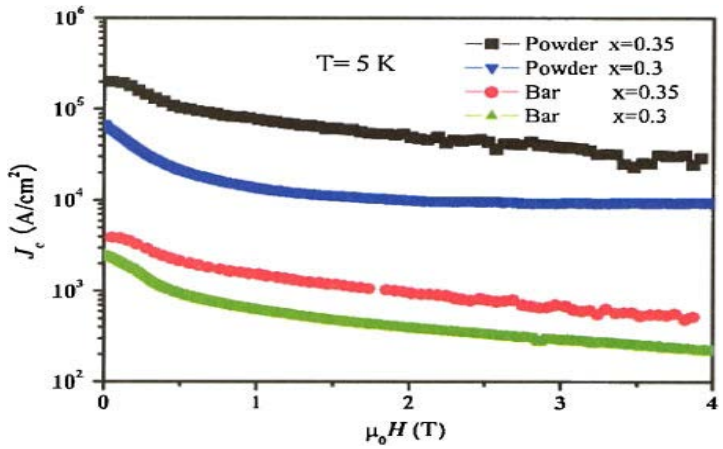

Figure 15: Magnetic field dependence of J_c at 5K for a bar and powder of F-Sm1111 PIT wires

4.2 Films on technical substrates

After high-J_c epitaxial thin films, especially those of 122 and 11 type compounds, were prepared on various singlecrystal substrates, the trial fabrication of their thin films on technical substrates such as flexible metal tapes with biaxially textured buffer layers has recently been reported. By employing the Fe buffer architecture, Iida and his colleagues realized the biaxially textured growth of Co-Ba122 thin films on IBAD-MgO-buffered Hastelloy substrates, [88] which are typically used for the fabrication of coated conductors. The films exhibited in-plane misorientation $\Delta\Phi$ of about 5.1^0, which was slightly smaller than that of the homoepitaxial MgO/IBAD-

MgO layer. They also showed a broader transition width and a substantially lower self-field J_c than those for films on MgO single-crystal substrates, as shown in Figure17.

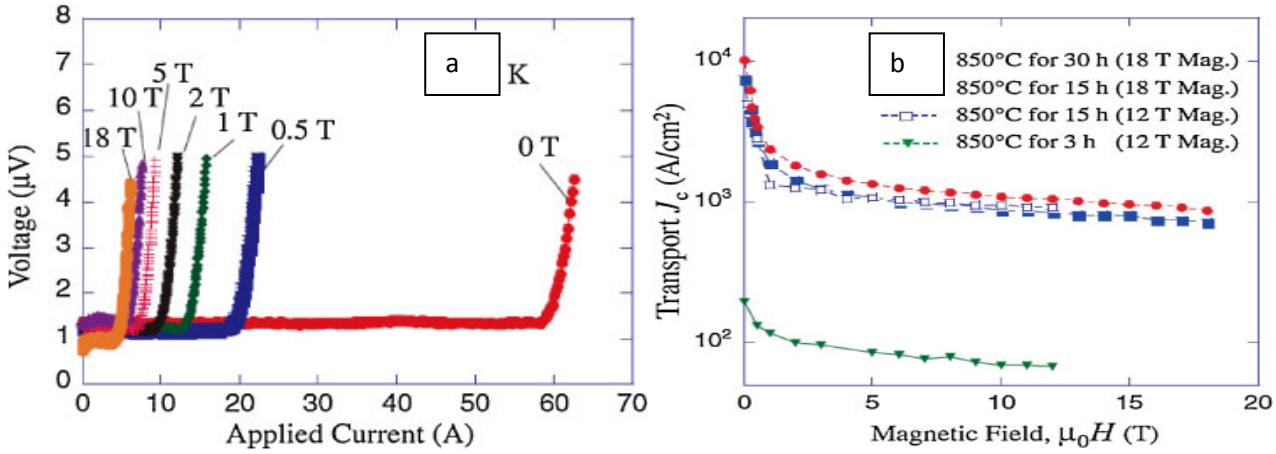

Figure 16: (Color online) (a) Typical voltage vs applied current curves measured for a K-Ba122 PIT wire heat-treated at 850 ^{0}C for 30 h. (b) Transport J_c as a function of applied magnetic field for the wires heat treated at 850 ^{0}C for 3, 15, and 30 h. Measurement was carried out in liquid helium (4.2 K) using an 18 T superconducting magnet.

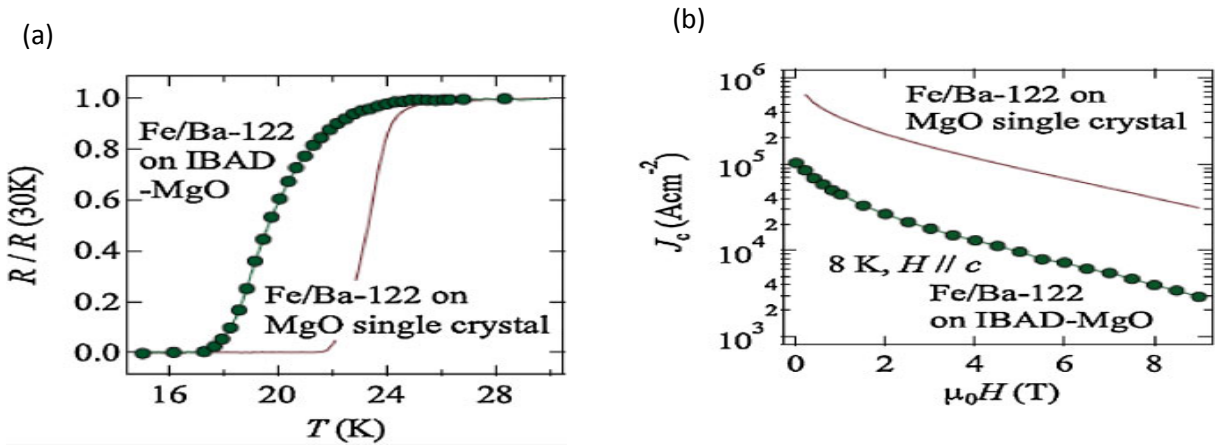

Figure 17: (Color online) (a) Normalized resistance of a Co-Ba122 thin film on IBAD-MgO. The data were normalized to the value at 30 K. For comparison, the resistance of a film on an MgO single-crystal substrate is also plotted. (b) J_c–H characteristics for the Co-Ba122 thin film on IBAD-MgO at 8K

On the other hand, Katase and his colleagues directly prepared biaxially textured Co-Ba122 thin films on IBAD-MgO buffered Hastelloy substrates [89]. Interestingly, the films showed a small in-plane misorientation $\Delta\Phi$ of approximately 3^0, despite the two times larger misorientation of the MgO base layers ($\Delta\Phi$ = 7.3^0). They exhibited a resistive transition as sharp as that for films on MgO single crystal substrates and high self-field J_c values of 1.2–3.6MA/cm^2 at 2K, as shown in Figure 18. These results imply that high-J_c Co-Ba122 coated

conductors can be fabricated by a rather simple low-cost process using less well textured templates with a large $\Delta\Phi$, although further technical challenges are required toward realizing practical tapes such as an improvement in the vortex pinning properties by the introduction of suitable pinning centers and the enhancement of material T_c values. The fabrication of Fe (Se,Te) 11 type compound thin films on IBAD-MgO-buffered Hastelloy substrates and rolling-assisted biaxially textured substrates (RABiTS) has also been reported by Li et al [90].

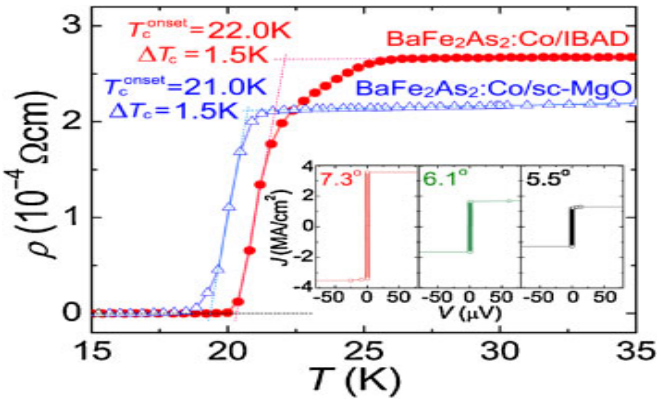

Figure 18: ρ –T curves for Co-Ba122 thin films on IBAD-MgO substrate (circles) and single-crystal MgO (triangles). The inset shows the *J*–V characteristics at 2K of the films on IBAD-MgO with (left) $\Delta\Phi_{MgO} = 7.3^0$, (middle) 6.1^0, and (right) 5.5^0

They found an enhancement of T_c onset up to 20K for the Fe (Se,Te) films. They have also reported a nearly isotropic J_c of over 10^4 A/cm^2 at 4.2K under a magnetic field as high as 25 T, indicating the high potential of the iron-based superconductor for future high field applications [91]. Co-doped Ba122 films with a high self-field J_c of over 1MA/cm^2 at low temperatures have been demonstrated. Further improvement of J_c, preferably in high magnetic fields and at moderately high temperatures, by optimizing flux pinning centers and/or microstructures is required for the development of practical wires or tapes. Although most of the above-mentioned demonstrations have been carried out using Co-doped Ba122 with a T_c of approximately 22 K, the application of iron-based superconductors with higher T_c values but similarly small anisotropy is desirable.

5. Conclusion

In summary we conclude hat, the iron-based superconductors promise interesting physics and applications. In this paper we briefly reviewed electronic, magnetic, and superconducting properties of iron-pnictide and iron-chalcogenide superconductors and their undoped parent compounds, covering only a small part of enormous works which have been achieved since 2008. Unlike high-T_c copper-oxide superconductors, electronic structures and magnetic properties of iron-based superconductors are quite well understood. Since electron-phonon interaction is too weak to explain the superconducting transition temperature as high as 55 K, the iron-based superconductors provide an excellent chance to understand an unconventional superconductivity which might be

helpful to reveal the origin of high-T_c superconductivity in copper oxides. Finally we have studied the applications of iron-based superconductors in wire and tapes which will help to produce industrial products. We hope that the topics described in this overview will be helpful for the researcher to do research and discover many new practical and possible applications of iron-based superconductors. The discovery of this new class of superconductors based on iron has tremendously revitalized the field of superconductivity, and should provide many more surprises and promises for the future.

References

[1] J. G. Bednorz and K. A. Müller, "Possible high T_c superconductivity in the Ba-La-Cu-O system", Z. Phys. B 64, 189-193 (1986).

[2] Y. Kamihara and his colleagues , "Iron-based layered superconductor: LaOFeP", J. Am. Chem. Soc. 128, 10012-10013 (2006).

[3] Y. Kamihara, T. Watanabe, M. Hirano, and H. Hosono,"Iron-based layered superconductor La[$O_{1-x}F_x$]FeAs (x= 0.05-0.12) with T_c = 26 K", J. Am. Chem. Soc. 130,3296-3297 (2008).

[4] Kamihara, Y., and his colleagues (2006). Iron-based layered superconductor: LaOFeP. Journal of the American Chemical Society, 128, 10012–10013.

[5] Kamihara, Y., Watanabe, T., Hirano, M., & Hosono, H. (2008). Iron-based layered superconductor

La [$O_{1-x}F_x$]FeAs(x = 0.05 − 0.12) with Tc = 26K. Journal of the American Chemical Society, 130, 3296.

[6] Zhi-An, R., and his colleagues (2008). Superconductivity at 55 K in iron-based F-doped layered quaternary compound Sm[$O_{1-x}F_x$]FeAs. Chinese Physics Letters, 25, 2215.

[7] Rotter, M., Tegel, M., & Johrendt, D. (2008). Superconductivity at 38 K in the iron arsenide ($Ba_{1-x}K_x$)Fe_2As_2. Physical Review Letters, 101, 107006.

[8] H. Ogino and his colleagues , "Superconductivity at 17 K in (Fe_2P_2)($Sr_4Sc_2O_6$): a new superconducting layered pnictide oxide with a thick perovskite oxide layer",Supercond. Sci. Technol. 22, 075008 (2009).

[9] X. Zhu and his colleagues , "Transition of stoichiometric Sr_2VO_3FeAs to a superconducting state at 37.2 K",Phys. Rev. B 79, 220512(R) (2009).

[10] S. Sato and his colleagues , "Superconductivity in a new iron pnictide oxide (Fe_2As_2)($Sr_4(Mg,Ti)_2O_6$)", Supercond. Sci.Technol. 23, 045001 (2010).

[11] K.-W. Lee and W. E. Pickett, "Sr_2VO_3FeAs: a nanolayered bimetallic iron pnictide superconductor", Euro. Phys. Lett. 89, 57008 (2010).

[12] J. Guo and his colleagues , "Superconductivity in the iron selenide $K_xFe_2Se_2$ ($0 \leq x \leq 1.0$)", Phys. Rev. B 82, 180520(R) (2010).

[13] Y. Zhang and his colleagues , "Nodeless superconducting gap in $A_xFe_2Se_2$ (A=K, Cs) revealed by angle-resolved photoemission spectroscopy", Nature Mater. 10, 273-277 (2011).

[14] D. Mou and his colleagues , "Distinct Fermi surface topology and nodeless superconducting gap in a (Tl0.58Rb0.42) $Fe_{1.72}Se_2$ superconductor", Phys. Rev. Lett. 106, 107001 (2011).

[15] A. F. Wang and his colleagues , "Superconductivity at 32 K in single-crystalline $Rb_xFe_{2-y}Se_2$", Phys. Rev. B 83, 060512(R) (2011).

[16] Kamihara, Yoichi; Watanabe, Takumi; Hirano, Masahiro and Hosono, Hideo (2008). "Iron-Based Layered Superconductor $La[O_{1-x}F_x]FeAs$ (x = 0.05–0.12) with T_c = 26 K". Journal of the American Chemical Society 130 (11): 3296–3297. doi:10.1021/ja800073m. PMID 18293989

[17]Chen, X. H.; Wu, T.; Wu, G.; Liu, R. H.; Chen, H. and Fang, D. F. (2008). "Superconductivity at 43 K in $SmFeAsO_{1-x}F_x$". Nature 453 (7196): 761–762. Bibcode:2008Natur.453..761C. doi:10.1038/nature07045. PMID 18500328

[18] Ren, Zhi-An; Che, Guang-Can; Dong, Xiao-Li; Yang, Jie; Lu, Wei; Yi, Wei; Shen, Xiao-Li; Li, Zheng-Cai; Sun, Li-Ling; Zhou, Fang; Zhao, Zhong-Xian (2008). "Superconductivity and phase diagram in iron-based arsenic-oxides $ReFeAsO_{1-\delta}$ (Re = rare-earth metal) without fluorine doping". EPL (Europhysics Letters) 83: 17002. arXiv:0804.2582. Bibcode:2008EL.....8317002R. doi:10.1209/0295-5075/83/17002

[19]Rotter, Marianne; Tegel, Marcus and Johrendt, Dirk (2008). "Superconductivity at 38 K in the Iron Arsenide $(Ba_{1-x}K_x)Fe_2As_2$". Physical Review Letters 101 (10): 107006. arXiv:0805.4630. Bibcode:2008PhRvL.101j7006R. doi:10.1103/PhysRevLett.101.107006. PMID 18851249

[20] Sasmal, K.; Lorenz, Bernd; Guloy, Arnold M.; Chen, Feng; Xue, Yu-Yi; Chu, Ching-Wu (2008). "Superconducting Fe-Based Compounds $(A_{1-x}Sr_x)$ Fe_2As_2 with A=K and Cs with Transition Temperatures up to 37 K". Physical Review Letters 101 (10): 107007. Bibcode:2008PhRvL.101j7007S. doi:10.1103/physrevlett.101.107007. PMID 18851250

[21] Shirage, Parasharam Maruti; Miyazawa, Kiichi; Kito, Hijiri; Eisaki, Hiroshi; Iyo, Akira (2008). "Superconductivity at 26 K in $(Ca_{1-x}Na_x)Fe_2As_2$". Applied Physics Express 1: 081702. Bibcode:2008APExp...1h1702M. doi:10.1143/APEX.1.081702

[22] Wang, X.C.; Liu, Q.Q.; Lv, Y.X.; Gao, W.B.; Yang, L.X.; Yu, R.C.; Li, F.Y.; Jin, C.Q. (2008). "The superconductivity at 18 K in LiFeAs system". Solid State Communications 148 (11–12): 538–540. arXiv:0806.4688. Bibcode:2008SSCom.148..538W. doi:10.1016/j.ssc.2008.09.057.

[23] Pitcher, Michael J.; Parker, Dinah R.; Adamson, Paul; Herkelrath, Sebastian J. C.; Boothroyd, Andrew T.; Ibberson, Richard M.; Brunelli, Michela; Clarke, Simon J. (2008). "Structure and superconductivity of LiFeAs". Chemical Communications (45): 5918–20. doi:10.1039/b813153h. PMID 19030538.

[24] Tapp, Joshua H.; Tang, Zhongjia; Lv, Bing; Sasmal, Kalyan; Lorenz, Bernd; Chu, Paul C. W.; Guloy, Arnold M. (2008). "LiFeAs: An intrinsic FeAs-based superconductor with T_c=18 K". Physical Review B 78 (6): 060505. arXiv:0807.2274. Bibcode:2008PhRvB..78f0505T. doi:10.1103/PhysRevB.78.060505.

[25] Chu, C.W.; Chen, F.; Gooch, M.; Guloy, A.M.; Lorenz, B.; Lv, B.; Sasmal, K.; Tang, Z.J.; Tapp, J.H.; Xue, Y.Y. (2009). "The synthesis and characterization of LiFeAs and NaFeAs". Physica C: Superconductivity 469 (9–12): 326–331. arXiv:0902.0806. Bibcode:2009PhyC..469.326C. doi:10.1016/j.physc.2009.03.016.

[26] Parker, Dinah R.; Pitcher, Michael J. and Clarke, Simon J. (2008). "Structure and superconductivity of the layered iron arsenide NaFeAs". Chemical Communications 2189 (16): 2189. arXiv:0810.3214. doi:10.1039/B818911K

[27] Zhang, S. J.; Wang, X. C.; Liu, Q. Q.; Lv, Y. X.; Yu, X. H.; Lin, Z. J.; Zhao, Y. S.; Wang, L.; Ding, Y.; Mao, H. K.; Jin, C. Q. (2009). "Superconductivity at 31 K in the "111"-type iron arsenide superconductor $Na_{1-x}FeAs$ induced by pressure". EPL (Europhysics Letters) 88 (4): 47008. Bibcode:2009EL.....8847008Z. doi:10.1209/0295-5075/88/47008

[28] Deng, Z.; Wang, X. C.; Liu, Q. Q.; Zhang, S. J.; Lv, Y. X.; Zhu, J. L.; Yu, R. C.; Jin, C. Q. (2009). "A new "111" type iron pnictide superconductor LiFeP". EPL (Europhysics Letters) 87 (3): 37004. Bibcode:2009EL.....8737004D

[29] Stewart, G. R. (2011). "Superconductivity in iron compounds". Rev. Mod. Phys. 83 (4): 1589. Bibcode:2011RvMP...83.1589S. doi:10.1103/revmodphys.83.1589

[30] H. Takahashi and his colleagues , “Superconductivity at 43 K in an iron-based layered compound LaO1-xFxFeAs”, Nature (London) 453, 376-378 (2008).

[31] X. H. Chen and his colleagues , “Superconductivity at 43 K in SmFeAsO1-xFx”, Nature (London) 453, 761-762 (2008).

[32]Y. Kamihara and his colleagues , J. Am. Chem. Soc. 128, 10012 (2006).

[33] G. F. Chen and his colleagues , “Superconductivity at 41 K and its competition with spin-density-wave instability in layered CeO1-xFxFeAs”, Phys. Rev. Lett. 100, 247002 (2008).

[34] Z. A. Ren and his colleagues , “Superconductivity at 52 K in iron based F doped layered quaternary compound Pr [O1-xFx]FeAs”, Mater. Res. Innov. 12, 105-106 (2008).

[35] K. Miyazawa and his colleagues , “Superconductivity above 50 K in LnFeAsO1-y (Ln=Nd, Sm, Gd, Tb, and Dy) synthesized by high-pressure technique”, J. Phys. Soc. Jpn. 78, 034712 (2009).

[36] Z.-A. Ren and his colleagues , “Superconductivity at 55 K in iron-based F-doped layered quaternary compound Sm[O1-xFx]FeAs”, Chin. Phys. Lett. 25, 2215-2216 (2008).

[37] C. de la Cruz and his colleagues , “Magnetic order close to superconductivity in the iron-based layered $LaO_{1-x}F_xFeAs$ systems”, Nature (London) 453, 899-902 (2008).

[38] N. Qureshi and his colleagues , “Crystal and magnetic structure of the oxypnictide superconductor LaFeAsO1-xFx: a neutron-diffraction study”, Phys. Rev. B 82, 184521 (2010).

[39] J. Zhao and his colleagues , “Structural and magnetic phase diagram of CeFeAsO1-xFx and its relation to high-temperature superconductivity”, Nature Mater 7, 953-959 (2008).

[40] M. Putti, I. Pallecchi, E. Bellingeri, M. R. Cimberle, M. Tropeano, C. Ferdeghini, A. Palenzona, C. Tarantini, A. Yamamoto, J. Jiang, J. Jaroszynski, F. Kametani, D. Abraimov, A. Polyanskii, J. D. Weiss, E. E. Hellstrom, A. Gurevich, D. C. Larbalestier, R. Jin, B. C. Sales, A. S. Sefat, M. A. McGuire, D. Mandrus, P. Cheng, Y. Jia, H. H. Wen, S. Lee, and C. B. Eom: Supercond. Sci. Technol. 23 (2010) 034003.

[41] J. Jaroszynski, F. Hunte, L. Balicas, Y.-J. Jo, I. Raic˘evic´, A. Gurevich, D. C. Larbalestier, F. F. Balakirev, L. Fang, P. Cheng, Y. Jia, and H. H. Wen: Phys. Rev. B 78 (2008) 174523.

[42] Z. S. Wang, H. Q. Luo, C. Ren, and H. H. Wen: Phys. Rev. B 78 (2008) 140501.

[43] M. Rotter, M. Tegel, and D. Johrendt, “Superconductivity at 38 K in the iron arsenide $(Ba_{1-x}K_x)Fe_2As_2$”, Phys. Rev. Lett. 101, 107006 (2008).

[43] X. C. Wang and his colleagues , “The superconductivity at 18 K in LiFeAs system”, Solid State Commun. 148, 538-540 (2008).

[44] R. Mittal and his colleagues , “Phonon dynamics in $Sr_{0.6}K_{0.4}Fe_2As_2$ and $Ca_{0.6}Na_{0.4}Fe_2As_2$ from neutron scattering and lattice-dynamical calculations”, Phys. Rev. B 78, 224518 (2008).

[45] R. Cortes-Gil and S. J. Clarke, “Structure, magnetism, and superconductivity of the layered iron arsenides $Sr_{1-x}NaxFe_2As_2$”, Chem. Mater. 23, 1009-1016 (2011).

[46] F.-C. Hsu and his colleagues , “Superconductivity in the PbO-type structure α-FeSe”, Proc. Natl. Acad. Sci. U.S.A. 105, 14262-14264 (2008).

[47] M. Rotter, M. Pangerl, M. Tegel, and D. Johrendt, “Superconductivity and crystal structures of $(Ba_{1-x}K_x)Fe_2As_2$ (x=0–1)”, Angew. Chem. Int. Ed. 47, 7949-7952 (2008). “Superconductivity and crystal structures of $(Ba_{1-x}K_x)Fe_2As_2$ (x=0–1)”, Angew. Chem. Int. Ed. 47, 7949-7952 (2008).

[48] N. Ni and his colleagues , “Effects of Co substitution on thermodynamic and transport properties and anisotropic H_{c2} in $Ba(Fe_{1-x}Co_x)_2As_2$ single crystals”, Phys. Rev. B 78, 214515 (2008).

[49] S. Jiang and his colleagues , “Superconductivity up to 30 K in the vicinity of the quantum critical point in $BaFe_2(As_{1-x}P_x)_2$”, J. Phys.: Condens. Matter 21,382203 (2009).

[50] J. Paglione and R. L. Greene, “High-temperature superconductivity in iron-based materials”, Nature Phys. 6, 645-658 (2010).

[51] T. Park and his colleagues , “Pressure-induced superconductivity in $CaFe_2As_2$”, J. Phys.: Condens. Matter 20, 322204 (2008).

[52] N. Doiron-Leyraud and his colleagues , “Quantum oscillations and the Fermi surface in an underdoped high-Tc superconductor”, Nature (London) 447, 565-568(2007).

[53] B. Maiorov, T. Katase, S. A. Baily, H. Hiramatsu, T. G. Holesinger, H. Hosono, and L. Civale: Supercond. Sci. Technol. 24 (2011) 055007.

[54] F.-C. Hsu and his colleagues , “Superconductivity in the PbO-type structure α-FeSe”, Proc. Natl. Acad. Sci. U.S.A. 105, 14262-14264 (2008).

[55] S. Medvedev and his colleagues , “Electronic and magnetic phase diagram of β-Fe1.01Se with superconductivity at 36.7 K under pressure”, Nature Mater. 8, 630-633 (2009).

[56] B. C. Sales and his colleagues , “Bulk superconductivity at 14 K in single crystals of Fe1+yTexSe1-x”, Phys. Rev. B 79, 094521 (2009).

[57] R. Hu, E. S. Bozin, J. B. Warren, and C. Petrovic, “Superconductivity, magnetism, and stoichiometry of single crystals of Fe1+y(Te1-xSx)z”, Phys. Rev. B 80, 214514 (2009).

[58] Y. Mizuguchi, F. Tomioka, S. Tsuda, T. Yamaguchi, and Y. Takano, “Superconductivity in S-substituted FeTe”, Appl. Phys. Lett. 94, 012503 (2009).

[59] J. H. Tapp, Z. Tang, B. Lv, K. Sasmal, B. Lorenz, C. W. Chu, and A. M. Guloy: Phys. Rev. B 78 (2008) 060505.

[60] J. Shimoyama, K. Kitazawa, K. Shimizu, S. Ueda, S. Horii, N. Chikumoto, and K. Kishio: J. Low Temp. Phys. 131 (2003) 1043.

[61] H. Ogino, S. Sato, N. Kawaguchi, Y. Shimizu, K. Machida, A.Yamamoto, K. Kishio, and J. Shimoyama: presented at Int. Workshop Novel Superconductors and Super Materials, 2011 (N2S2011).

[62] X. Wang, Q. Q. Liu, Y. X. Lv, W. B. Gao, L. X. Yang, R. C. Yu, F. Y. Li, and C. Q. Jin, Solid State Commun. 148, 538 (2008).

[63] J. H. Tapp, Zh. Tang, B. Lv, K. Sasmal, B. Lorenz, P. C. W. Chu, and A. M. Guloy, Phys. Rev. B 78, 060505 (2008).

[64] S. V. Borisenko, V. B. Zabolotnyy, D. V. Evtushinsky, T. K. Kim, I. V. Morozov, A. N. Yaresko, A. A. Kordyuk, G. Behr, A. Vasiliev, R. Follath, and B. B€uchner, Phys. Rev. Lett. 105, 067002 (2010).

[65] A. A. Kordyuk, V. B. Zabolotnyy, D. V. Evtushinsky, T. K. Kim, I. V. Morozov, M. L. Kulic´, R. Follath, G. Behr, B. B€uchner, and S. V. Borisenko, Phys. Rev. B 83, 134513 (2011).

[66]S. V. Borisenko, V. B. Zabolotnyy, A. A. Kordyuk, D. V. Evtushinsky, T. K. Kim, I. V. Morozov, R. Follath, and B. B€uchner, Symmetry 4, 251 (2012).

[67] I. Morozov, A. Boltalin, O. Volkova, A. Vasiliev, O. Kataeva, U. Stockert, M. Abdel-Hafiez, D. Bombor, A. Bachmann, L. Harnagea, M. Fuchs, H.-J. Grafe, G. Behr, R. Klingeler, S. Borisenko, Ch. Hess, S. Wurmehl, and B. B€uchner, Cryst. Growth Des. 10, 4428 (2010).

[68] G. F. Chen, W. Z. Hu, J. L. Luo, and N. L. Wang, Phys. Rev. Lett. 102, 227004 (2009).

[69] S. Li, C. de la Cruz, Q. Huang, G. F. Chen, T.-L. Xia, J. L. Luo, N. L. Wang, and P. Dai, Phys. Rev. B 80, 020504 (2009).

[70]M. A. Tanatar, N. Spyrison, K. Cho, E. C. Blomberg, G. Tan, P. Dai, Ch. Zhang, and R. Prozorov, Phys. Rev. B 85, 014510 (2012).

[71]D. R. Parker, M. J. P. Smith, T. Lancaster, A. J. Steele, I. Franke, P. J. Baker, F. L. Pratt, Michael J. Pitcher, S. J. Blundell, and Simon J. Clarke, Phys. Rev. Lett. 104, 057007 (2010).

[72] C. He, Y. Zhang, B. P. Xie, X. F. Wang, L. X. Yang, B. Zhou, F. Chen, M. Arita, K. Shimada, H. Namatame, M. Taniguchi, X. H. Chen, J. P. Hu, and D. L. Feng, Phys. Rev. Lett. 105, 117002 (2010).

[73] C. He, Y. Zhang, X. F. Wang, J. Jiang, F. Chen, L. X. Yang, Z. R. Ye, Fan Wu, M. Arita, K. Shimada, H. Namatame, M. Taniguchi, X. H. Chen, B. P. Xie, and D. L. Feng, J. Phys. Chem. Solids 72, 479 (2011).

[74] K. Segawa and Y. Ando, J. Phys. Soc. Jpn. 78, 104720 (2009). 73B. C. Sales, A. S. Sefat, M. A. McGuire, R. Y. Jin, D. Mandrus

[75] G. Osabe, N. Ayai, M. Kikuchi, K. Tatamidani, T. Nakashima, J. Fujikami, T. Kagiyama, K. Yamazaki, S. Yamade, E. Shizuya, S. Kobayashi, K. Hayashi, K. Sato, J. Shimoyama, H. Kitaguchi, and H. Kumakura: Physica C 470 (2010) 1365.

[76] Z. Gao, L. Wang, Y. Qi, D. Wang, X. Zhang, and Y. Ma: Supercond. Sci. Technol. 21 (2008) 105024.

[77] Z. Gao, L. Wang, Y. Qi, D. Wang, X. Zhang, Y. Ma, H. Yang, and H. Wu: Supercond. Sci. Technol. 21 (2008) 112001.

[78] Y. Qi, X. Zhang, Z. Gao, Z. Zhang, L. Wang, D. Wang, and Y. Ma: Physica C 469 (2009) 717.

[79] L. Wang, Y. Qi, D. Wang, X. Zhang, Z. Gao, Z. Zhang, Y. Ma, S. Awaji, G. Nishijima, and K. Watanabe: Physica C 470 (2010) 183.

[80] Y. Qi, L. Wang, D. Wang, Z. Zhang, Z. Gao, X. Zhang, and Y. Ma: Supercond. Sci. Technol. 23 (2010) 055009.

[81] Y. Ma, L. Wang, Y. Qi, Z. Gao, D. Wang, and X. Zhang: IEEE Trans. Appl. Supercond. 21 (2011) 2878.

[82] K. Togano, A. Matsumoto, and H. Kumakura: Appl. Phys. Express 4 (2011) 043101.

[83] M. Fujioka, T. Kota, M. Matoba, T. Ozaki, Y. Takano, H. Kumakura, and Y. Kamihara: Appl. Phys. Express 4 (2011) 063102.

[84] L. Wang, Y. Ma, Q. Wang, K. Li, X. Zhang, Y. Qi, Z. Gao, X. Zhang, DWang, C. Yao, and C. Wang: Appl. Phys. Lett. 98 (2011) 222504

[85] Y. Mizuguchi, K. Deguchi, S. Tsuda, T. Yamaguchi, H. Takeya, H. Kumakura, and Y. Takano: Appl. Phys. Express 2 (2009) 083004.

[86] T. Ozaki, K. Deguchi, Y. Mizuguchi, H. Kumakura, and Y. Takano: IEEE Trans. Appl. Supercond. 21(2011) 2858.

[87] T. Ozaki, K. Deguchi, Y. Mizuguchi, Y. Kawasaki, T. Tanaka, T. Yamaguchi, H. Kumakura, and Y. Takano: to be published in J. Appl.Phys.

[88] K. Iida, J. Ha¨nisch, S. Trommler, V. Matias, S. Haindl, F. Kurth, I. L. del Pozo, R. Hu¨hne, M. Kidszun, J. Engelmann, L. Schultz, and B. Holzapfel: Appl. Phys. Express 4 (2011) 013103.

[89] T. Katase, H. Hiramatsu, V. Matias, C. Sheehan, Y. Ishimaru, T. Kamiya, K. Tanabe, and H. Hosono: Appl. Phys. Lett. 98 (2011) 242510.

[90] Q. Li, W. Si, Q. Jie, J. Zhu, S. Solovyov, A. Goyal, and V. Matias: presented at Applied Superconductivity Conf., 2010 (ASC2010).

[91] W. Si, J. Zhou, Q. Jie, I. Dimitrov, V. Solovyov, P. D. Johnson, J. Jaroszynski, V. Matias, C. Sheehan, and Q. Li: Appl. Phys. Lett. 98 (2011) 262509.